Reprinted from ENVIRONMENTAL SCIENCE & TECHNOLOGY, Vol. 23, Page 451, April 1989

Technique for Measuring the Indoor ^{222}Rn Source Potential of Soil

William W. Nazaroff*

Indoor Environment Program, Applied Science Division, Lawrence Berkeley Laboratory, and Department of Civil Engineering, University of California, Berkeley, California 94720

Richard G. Sextro

Indoor Environment Program, Applied Science Division, Lawrence Berkeley Laboratory, University of California, Berkeley, California 94720

■ Elevated indoor ^{222}Rn concentrations are often caused by high rates of entry from soil. The ^{222}Rn source potential of soil depends on two parameters: the release rate of ^{222}Rn into the soil pores and the volume of soil that can contribute its emanated ^{222}Rn to indoor air. These parameters are characterized, respectively, by the soil's ^{222}Rn generation rate and its permeability. By measuring two quantities associated with air extracted from a soil probe—the ^{222}Rn concentration and the flow rate associated with a specified dynamic pressure difference—both characteristics may be determined from a single procedure. A means of interpreting results from the probe technique to predict ^{222}Rn entry potential into a basement with a perimeter leakage path is provided. In a field test of the technique, the measured ^{222}Rn source potential in soils adjacent to a sample of four houses correlates well with measured indoor ^{222}Rn concentrations.

Introduction

Exposure to ^{222}Rn decay products in indoor air is now broadly recognized as a major environmental concern. A central element in any strategy for controlling exposure is the identification of buildings with elevated concentrations. The wide range of indoor concentrations that has been observed is largely due to differences among buildings in the rate of ^{222}Rn entry, particularly from underlying soil which appears to be the predominant source in most houses with elevated levels (*1*, *2*).

The importance of soil as a source of indoor ^{222}Rn, combined with the observed geographic clustering of high indoor concentrations (*3*, *4*), suggests that an appraisal of soil-related factors may be sufficient to determine the potential of an area to have high indoor concentrations. Such an appraisal could constitute the basis for prioritizing efforts to identify individual houses with high concentrations; it could also be used to determine whether construction practices in an area need to be modified to prevent elevated concentrations in future housing. Prior work on this topic has not yet yielded widely used methods (*5*–*7*).

In this paper, a technique is presented for measuring the key soil parameters—permeability and the rate of release of ^{222}Rn into the soil pores—and combining them to determine the soil's ^{222}Rn source potential. Results of measuring the source potential and indoor concentrations of ^{222}Rn at four sites in New Jersey provide a preliminary demonstration of the efficacy of the technique.

Radon Source Potential

The ^{222}Rn source potential, as defined here, is a parameter designed to indicate the level of risk of high indoor ^{222}Rn concentrations in buildings constructed on a given soil. More specifically, it is an estimate of the maximum sustainable rate of entry of ^{222}Rn from the soil into a building, with units of activity per time (i.e., Bq s^{-1}).

Two key characteristics determine the ^{222}Rn source potential of a soil: the rate of release of ^{222}Rn atoms from the soil grains into its pore space and the volume of soil that can make a sustained contribution of ^{222}Rn to indoor air. The first of these depends primarily on the content and distribution of ^{226}Ra within the soil grains. This characteristic also varies with environmental conditions—notably soil moisture content—which can affect the fraction of radon produced that enters the pore space of the soil (*8*). The second characteristic depends on the resistance of the soil to radon migration and on properties of the interface between the building and the soil, such as the geometry of the building substructure and the location of transport paths across the substructure shell.

The technique proposed here entails installing a sampling probe into the soil. A pump is used to establish a reduced dynamic air pressure in the probe, relative to the atmosphere. The resulting air flow rate through the probe is measured, serving as a basis for computing soil permeability. A sample of the extracted air is analyzed to determine its ^{222}Rn content; from this measurement, the rate of release of ^{222}Rn into the soil pores can be determined. The measurement results are combined according to the method developed below to compute the ^{222}Rn source potential.

To implement the method, it is necessary to make assumptions about characteristics of the soil, about the nature of ^{222}Rn transport processes in the soil, and about characteristics of the building. For the purposes of this paper, we make the following primary assumptions, designed to capture the dominant features of ^{222}Rn transport and entry that lead to high indoor concentrations while retaining enough simplicity for the analysis to be tractable: (i) the soil has uniform and isotropic properties, (ii) molecular diffusion can be neglected compared with bulk air flow as a ^{222}Rn transport process through the soil pores, and (iii) the building has a basement substructure with a penetration to the soil near the level of the floor that extends around the building perimeter and has uniform width. These assumptions are discussed in subsequent sections. To obtain numerical values of the ^{222}Rn source potential, one must specify specific structural dimensions. We assume values corresponding to a typical single-family residence in the United States: that the basement perimeter is 40 m, and that the floor is 2 m below the soil surface. Results are computed for two values of the width of the perimeter penetration approximately spanning the expected range of conditions: (i) 0.1 cm, corresponding to a shrinkage crack in the concrete floor and (ii) 15 cm, corresponding to a perimeter drain tile system plus gravel. (It shall be seen that radon entry is relatively insensitive to penetration width: although these widths differ by a factor of 150, the corresponding source potentials differ only by a factor of approximately 2.) One must also specify a nominal dynamic pressure difference from outdoors to

0013-936X/89/0923-0451$01.50/0

inside that can cause air flow through the soil; we assume 4 Pa (see, e.g., ref 9). Additional assumptions are introduced as needed throughout the course of the paper.

We emphasize that the ^{222}Rn source potential of soil is inextricably linked to a conceptual description of a building's substructure, particularly the manner in which it is coupled to the soil. We view this linkage as necessary, because the transport of radon in soil near a building is strongly influenced by the building itself. Because of this linkage, it may be necessary to modify the interpretive aspects of this technique if the characteristics of a building of interest differ markedly from those assumed here or if future research demonstrates that the transport paths and mechanisms assumed here are not the dominant ones in the housing stock.

Radon Production and Transport in Soil

In this section a theoretical description of ^{222}Rn transport in soil is presented and the condition necessary to justify the assumption that diffusion may be neglected is derived. The equations presented here serve as the basis for the source-potential measurement technique.

The general transport equation describing the rate of change of radon concentration in a differential element of the soil pore air is (*10*)

$$\frac{\partial I}{\partial t} = \frac{1}{\epsilon}\vec{\nabla}\cdot D\vec{\nabla}I - \frac{1}{\epsilon}\vec{\nabla}\cdot I\vec{v} + G - \lambda I \qquad (1)$$

where I is the ^{222}Rn activity concentration in the soil pores, ϵ is the soil porosity, D is the molecular diffusion coefficient of ^{222}Rn in soil air (relating the gradient of the interstitial concentration to the flux density across the total geometric area), $\vec{v}$ is the Darcian velocity vector (i.e., the flux density of soil air divided by the total geometric area), G is the release rate of ^{222}Rn from soil grains into the pore air, and λ is the radioactive decay constant of ^{222}Rn. (For flows much larger than those of interest here, the molecular diffusion coefficient is replaced by a coefficient of flow dispersion; see, e.g., ref 11.) On the right-hand side, the terms account for diffusive transport, convective transport, generation, and decay, respectively, of ^{222}Rn. It is assumed throughout this paper that the moisture content of the soil pores is small enough so that dissolved ^{222}Rn may be neglected. (This point is discussed further in ref 8.) The ^{222}Rn generation rate, G, is related to more fundamental parameters by the expression

$$G = f\rho_s A_{Ra}\lambda(1 - \epsilon)/\epsilon \qquad (2)$$

where f is the emanation coefficient (i.e., the fraction of radon atoms produced in the soil grains that enter the interstitial pore space before decaying), ρ_s is the density of the soil grains (commonly 2.65×10^3 kg m^{-3}), and A_{Ra} is the ^{226}Ra content of the soil.

In the analysis here, it is assumed that $\vec{v}$ is described by Darcy's law:

$$\vec{v} = -(k/\mu)\vec{\nabla}P \qquad (3)$$

where k is the intrinsic permeability of the soil, μ is the dynamic viscosity of the air in the soil pores, and $\vec{\nabla}P$ is the gradient of the dynamic pressure. For this description to be valid, several conditions must be satisfied. The soil must be isotropic with respect to permeability. The Reynolds number ($d_g v/\nu$, where d_g is a characteristic dimension of the soil grains and ν is the kinematic viscosity of air) must be sufficiently small (less than approximately 4) that the flow is in the laminar–linear regime (*12*). The pore size must be large relative to the mean free path of the gas molecules (~0.065 μm at 20 °C). For the problem of ^{222}Rn migration in soil, these conditions are usually satisfied; however, in using the technique described in this paper, one must take care to ensure that the upper limit on the Reynolds number is not exceeded, otherwise the assumption necessary for Darcy's law to apply—that the fluid drag is proportional to the mean fluid velocity through the soil column—doesn't hold.

Pressure disturbances associated with ^{222}Rn migration in soil are a small fraction of the atmospheric pressure (e.g., ref 8 and 9); consequently we shall treat air as an incompressible fluid. In this case, under steady-state conditions, $\vec{\nabla}\cdot\vec{v} = 0$, and so, assuming the soil is isothermal and its permeability is isotropic and homogeneous, the dynamic pressure satisfies the Laplace equation:

$$\nabla^2 P = 0 \qquad (4)$$

By making the further assumption that the diffusion coefficient is spatially constant, eq 1 becomes

$$\frac{\partial I}{\partial t} = D_e\nabla^2 I + \frac{k}{\epsilon\mu}\vec{\nabla}P\cdot\vec{\nabla}I + G - \lambda I \qquad (5)$$

where $D_e = D/\epsilon$ is the effective coefficient of molecular diffusion of radon in soil air.

Solving this equation is greatly simplified if one of the transport processes—advection or diffusion—may be neglected with respect to the other. To determine the circumstances in which this is possible, we multiply and divide each variable and operator in eq 5 by a unique combination of a characteristic time λ^{-1}, length H, and dynamic pressure difference ΔP_o as needed to make each dimensionless. The result is

$$\frac{1}{N_\tau}\frac{\partial I^*}{\partial t^*} = \frac{1}{\mathrm{Pe}_p}\nabla^{*2} I^* + \vec{\nabla}^* P^*\cdot\vec{\nabla}^* I^* + \frac{1}{N_\tau}(G^* - I^*) \qquad (6)$$

where the asterisks denote dimensionless quantities, which, if the characteristic parameters are chosen properly, have unit order of magnitude. This equation has two dimensionless groups

$$\mathrm{Pe}_p = \epsilon k\Delta P_o/\mu D_e \qquad (7)$$

and

$$N_t = k\Delta P_o/\epsilon\mu\lambda H^2 = \Pi_2 \qquad \text{(see Table I)} \qquad (8)$$

The group Pe_p is effectively a Pĕclet number for mass transfer in a porous medium. It gives the ratio of the characteristic velocity of advection to that due to diffusion. In cases in which the ^{222}Rn entry rate from a uniform soil is high, advection dominates diffusion as a ^{222}Rn transport process (e.g., ref 1, 2, 9, and 13). For assessing the ^{222}Rn source potential, whereby we seek to identify soils with potential for generating high entry rates, molecular diffusion is neglected. Strictly, to be able to neglect diffusion, the condition $\mathrm{Pe}_p \gg 1$ must be satisfied. For radon entry into a house, typical parameter values are $\Delta P_o = 4$ Pa, $\epsilon = 0.5$, $\mu = 17 \times 10^{-6}$ kg m^{-1} s^{-1}, and $D_e = 2 \times 10^{-6}$ m^2 s^{-1} (*8*). In this case $\mathrm{Pe}_p = 1$ if $k = 1.7 \times 10^{-11}$ m^2. So, for soils with much larger permeability—i.e., uniform medium to coarse sands and gravels, or smaller grained soils with large structural permeabilities—transport by molecular diffusion may be neglected.

Finally, we assume that steady-state conditions prevail. Under these conditions (again neglecting diffusion), the governing equation for ^{222}Rn concentration in the soil pores, in dimensional form, is

$$-(\vec{v}/\epsilon)\cdot\vec{\nabla}I + G - \lambda I = 0 \qquad (9)$$

This equation will be solved numerically below to evaluate radon entry by pressure-driven flow into a building.

To correctly interpret the results from the sampling probe, we also need to consider the case of radon migration in soil far from structures. Evidence suggests that transport by molecular diffusion dominates in this case, although rainfall and variations in barometric pressure have substantial influence at times (*14*). By neglecting convective flow for the case of uncovered soil of infinite depth and extent and assuming the radon concentration to be zero at the soil surface, the steady-state solution to the one-dimensional form of eq 5 yields the radon activity concentration in the soil pores at a depth z below the surface:

$$I(z) = (G/\lambda)(1 - e^{-z/l_D}) \tag{10}$$

where $l_D = (D_e/\lambda)^{1/2}$ is known as the diffusion length.

Analysis for a Spherical Cavity

Introduction. The sampling technique, described in detail in a subsequent section, is designed to generate a small spherical cavity in the soil at the end of a sampling probe. To correctly interpret the measurement results, it is essential to consider the dynamic response of air in the soil pores, and of ^{222}Rn within the pore air, to the withdrawal of air through the probe. The measurement system is modeled as an isolated spherical cavity buried in a semiinfinite, homogeneous, isotropic, and uniform soil. The temporal response of this system can be considered to have three periods: (i) an initial interval during which the pressure in the soil pores is changing with time in response to the sudden depressurization of the cavity; (ii) an intermediate interval during which pressure and flow conditions are steady, but the radon concentration in the soil pores is changing; and (iii) the steady-state period. The characteristic time, t_p, associated with the initial interval is given by (*8*, *15*)

$$t_p = \mu\epsilon H^2/k P_a \tag{11}$$

where H is the depth of the center of the cavity below the soil surface and P_a is the atmospheric pressure. A representative value of t_p is 9 s for a soil having a permeability of 10^{-11} m^2 and a cavity depth of 1 m. The characteristic time to reach period iii is the minimum of (a) the characteristic time for a parcel of air to travel from the soil surface to the cavity or (b) the half-life of ^{222}Rn (3.8 days). In either case, it is much longer than the duration of period i. As will be seen in the discussion of Figure 1 to follow, the time to achieve steady state for a representative case is on the order of days. Thus, the most practical approach to sampling for the ^{222}Rn source potential is to measure the flow and pressure difference during the early part of period ii and to measure the ^{222}Rn content of air sampled from the immediate vicinity of the soil probe. The interpretation of these results in terms of soil permeability and radon generation rate are described in the following subsection. The steady-state period is analyzed subsequently.

Interpretation of Sampling Probe Data. The dynamic pressure difference across the soil and the flow rate into the cavity are used to determine the soil permeability in the following manner. First, the Laplace equation (eq 4) is solved subject to the boundary conditions that the dynamic pressure has a uniform value at the soil surface and a distinct uniform value within the cavity. Next, by means of eq 3, the fluid velocity in the soil is calculated and integrated over the surface of the cavity. This problem

Table I. Definition of Dimensionless Parameters

parameter	definition[a]	measurement of
Π_1	r/H	cavity size
Π_2	$\Delta P_o k/\epsilon\mu\lambda H^2$	pressure difference
Π_3	$F/\epsilon G H^3$	radon flux into spherical cavity
Π_4	$Q\mu/\Delta P_o k r$	air flow into spherical cavity
Π_5	$F/\epsilon G H^2 L$	radon flux into cylindrical cavity
Π_6	$Q\mu/\Delta P_o k L$	air flow into cylindrical cavity

[a] F is the radon activity flux into the cavity (Bq s^{-1}); G is the radon-222 release rate into the soil pores (Bq m^{-3} s^{-1}); H is the depth of the cavity center below the soil surface (m); k is the permeability of the soil (m^2); L is the axial length of the cylinder (m); ΔP_o is the dynamic pressure difference between the soil surface and the cavity (Pa); Q is the volumetric air flow rate into the cavity (m^3 s^{-1}); r is the radius of the cavity (m); ϵ is the porosity of the soil (–); λ is the radioactive decay constant of radon-222 (2.1×10^{-6} s^{-1}); μ is the dynamic viscosity of air (kg m^{-1} s^{-1}).

may be solved analytically by making a transformation of eq 3 to bispherical coordinates (*16*), with the result

$$\Pi_4 = 8\pi[(1/\Pi_1)^2 - 1]^{1/2} \sum_{n=0}^{\infty} \{[(1/\Pi_1) + \{(1/\Pi_1)^2 - 1\}^{1/2}]^{2n+1} - 1\}^{-1} \tag{12}$$

where Π_4 is a normalized rate of air flow and Π_1 is the normalized size of the cavity, as defined in Table I. In the limit $\Pi_1 \to 0$, $\Pi_4 = 4\pi$. For practical use, with $\Pi_1 \leq 0.2$, only the first term ($n = 0$) in the infinite sum need be evaluated; the error is less than 1%. The right-hand side may be evaluated for any probe dimensions; then, given the flow rate Q, and the pressure difference ΔP_o, the permeability k may be determined from the definition of Π_4.

The radon generation rate is determined from the measured radon concentration by using eq 10. The diffusion length of radon in soil varies from a few centimeters to a meter or more, depending largely on the soil moisture content (*7*, *8*, *17*). The unknown diffusion length may be determined by measuring the radon concentration at two different depths. It may also be determined by estimating the effective diffusion coefficient, D_e, based, for example, on separate measurements of porosity and moisture content of the soil and the following empirical correlation (ref 17; see also ref 7 and 8):

$$D_e = \gamma \exp[-4(m - m\epsilon^2 + m^5)] \tag{13}$$

where $\gamma = 7 \times 10^{-6}$ m^2 s^{-1} and m is the moisture saturation (fraction of the soil pore volume filled with water). If the cavity depth is sufficiently great relative to the expected diffusion length, the exponential term in eq 10 may simply be neglected.

Steady-State Analysis. If the transit time of parcels of air from the surface of the soil to the cavity is not large relative to the half-life of ^{222}Rn, the concentration of ^{222}Rn entering the cavity under steady-state conditions will be lower than the initial concentration. The results of the steady-state case are considered because, although the routine use of the measurement technique would be based on the short-term relationships given above, the steady-state case may be of use in research applications.

As stated in the previous subsection, the Laplace equation (eq 4) may be solved analytically to determine the dynamic pressure as a function of position in the soil. Darcy's law (eq 3) may then be used to calculate the velocity field. With this result, the normalized ^{222}Rn flux into the cavity, Π_3, is determined by solving eq 9 using a Lagrangian frame-of-reference to compute the ^{222}Rn concentration as a function of position over the surface of the

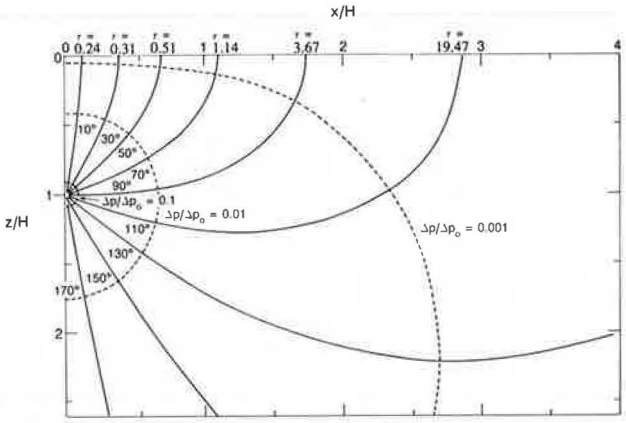

Figure 1. Flow trajectories and pressure field for a spherical cavity with $\Pi_1 = 0.01$ and $\Pi_2 = 100$ (see Table I for definition of parameters). The streamlines are labeled with the zenith angle at which they penetrate the cavity and with the normalized time of travel, $\tau = \lambda t$ where $\lambda = 2.1 \times 10^{-6}$ s^{-1} is the ^{222}Rn decay constant and t is the dimensional travel time. Note that τ is inversely proportional to Π_2.

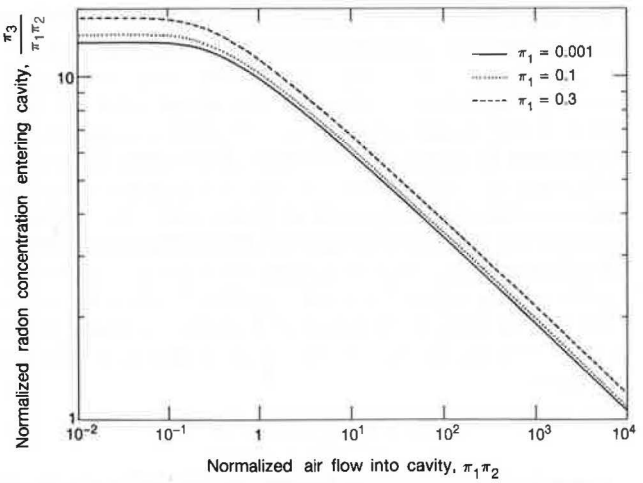

Figure 2. Normalized radon concentration entering a spherical cavity under steady-state conditions vs the normalized rate of air flow into the cavity. Results are plotted for three different values of Π_1, the ratio of cavity radius to depth.

cavity and then integrating the product of the ^{222}Rn concentration and the soil gas velocity over the cavity surface. The approach to computing the ^{222}Rn concentration at the cavity surface is most easily understood by considering a fluid streamline originating at the soil surface, traversing the soil, and entering the cavity. In the Lagrangian frame-of-reference, the origin of the coordinate system moves along the streamline at the rate of air flow. Because diffusion is neglected, the ^{222}Rn concentration at the origin of this reference system is governed only by the rates of production and radioactive decay in the soil pores. Thus, given the assumptions of soil homogeneity and negligible ^{222}Rn concentration in the air above the soil, the ^{222}Rn concentration at any point in the soil pores is simply

$$I = (G/\lambda)(1 - e^{-\lambda t}) \tag{14}$$

where t is the time of travel along the appropriate streamline from the soil surface to the given point.

Formally, eq 14 is obtained from eq 9 in the following manner. In the absence of diffusion, and for a uniform soil, the gradient of the ^{222}Rn concentration in the soil pores is parallel to the direction of air flow through the pores. Thus, $\vec{v}\cdot\vec{\nabla}I = v(\mathrm{d}I/\mathrm{d}s)$, where $\mathrm{d}s$ is a differential distance along a streamline. Furthermore, $v/\epsilon = \mathrm{d}s/\mathrm{d}t$. By use of these relationships, and the chain rule, eq 9 becomes

$$-(\mathrm{d}I/\mathrm{d}t) + G - \lambda I = 0 \tag{15}$$

With boundary condition $I = 0$ at $t = 0$ (i.e., at the soil surface), eq 14 is the solution to eq 15.

The problem has therefore been reduced to determining t as a function of position around the surface of the cavity. Since $\vec{v}$ is known as a function of position throughout the soil, t may be determined for any point on the cavity surface by integrating $\mathrm{d}\vec{s}/-\vec{v}$ along the streamline from the cavity to the soil surface. This integration was accomplished numerically, using a fourth-order Runge–Kutta method (*18*), applied at 1° intervals over the zenith angle.

The normalized time of travel along a given trajectory, $\tau(=\lambda t)$, scales linearly with the inverse of the Darcian velocity and, consequently, with the inverse of the normalized dynamic pressure difference, Π_2. Thus, for a given cavity geometry, Π_1, the trajectory travel times need only be computed for one value of Π_2; the times for any other value of Π_2 are obtained by a linear scaling.

To give an appreciation of the paths and travel times, several trajectories are plotted in Figure 1 for one case, $\Pi_1 = 0.01$ and $\Pi_2 = 100$. (For a typical deployment of the technique, with $H = 1.5$ m and $\Delta P_o = 50$ Pa, $\Pi_2 = 100$ for $k \sim 7 \times 10^{-11}$ m^2, equivalent to the permeability of a uniform, medium sand.) Two features of this figure are noteworthy. First, the dynamic pressure falls rapidly with distance from the cavity surface: 90% of the pressure drop is confined to a zone of approximate radius $0.1H$. Second, for these conditions, the normalized travel times for paths entering the upper portion of the cavity are O(1) i.e., the dimensional travel times are comparable to the ^{222}Rn half-life of 3.8 days.

The variation of the steady-state ^{222}Rn flux with cavity size and dynamic pressure difference is shown in Figure 2 for a broad range of conditions, under the assumption that $H \gg l_D$. There are two zones of interest. For small values of the product $\Pi_1\Pi_2$ ($\Pi_1\Pi_2 < 0.1$), the radon flux (Π_3) is roughly proportional to $\Pi_1\Pi_2$, and for small Π_1, the proportionality constant is 4π. In this region the long trajectory travel times imply that the ^{222}Rn concentration at all positions on the cavity surface is equal to the upper limit, G/λ. The ^{222}Rn flux is the product of this concentration and the air flow rate into the cavity. On the other hand, for large values of $\Pi_1\Pi_2$ ($\Pi_1\Pi_2 > 3$), the ^{222}Rn flux increases approximately as $(\Pi_1\Pi_2)^{3/4}$. In this region, the average ^{222}Rn concentration entering the cavity is lower than the G/λ limit because the normalized trajectory travel time, τ, is reduced to O(1) or less over a portion of the surface of the cavity.

The following empirical fit to the curves in Figure 2 yields values of Π_3 accurate to within 4% for $\Pi_1 < 0.1$, and for $\Pi_1\Pi_2 < 10^4$:

$$\log\left[\frac{\Pi_3}{\Pi_1\Pi_2}\right] = 1.111 \qquad \Pi_1\Pi_2 \le 0.1$$

$$\log\left[\frac{\Pi_3}{\Pi_1\Pi_2}\right] = 1.00 - 0.168\log(\Pi_1\Pi_2) - 0.055\log^2(\Pi_1\Pi_2) \qquad 0.1 < \Pi_1\Pi_2 \le 10$$

$$\log\left[\frac{\Pi_3}{\Pi_1\Pi_2}\right] = 1.0342 - 0.2495\log(\Pi_1\Pi_2) \qquad \Pi_1\Pi_2 > 10 \tag{16}$$

Analysis for a Cylindrical Cavity

Introduction. The spherical cavity is a poor representation of the substructure penetrations that commonly

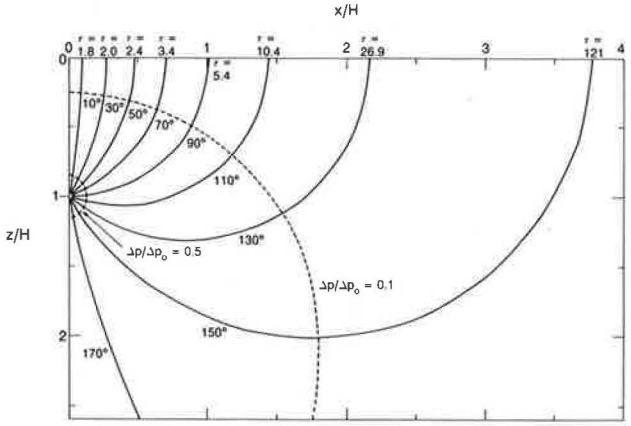

Figure 3. Flow trajectories and pressure field for a cylindrical cavity with $\Pi_1 = 0.01$ and $\Pi_2 = 1$ (see Table I for definition of parameters). The streamlines are labeled with the zenith angle at which they penetrate the cavity and with the normalized time of travel, $\tau = \lambda t$ where $\lambda = 2.1 \times 10^{-6}$ s^{-1} is the ^{222}Rn decay constant.

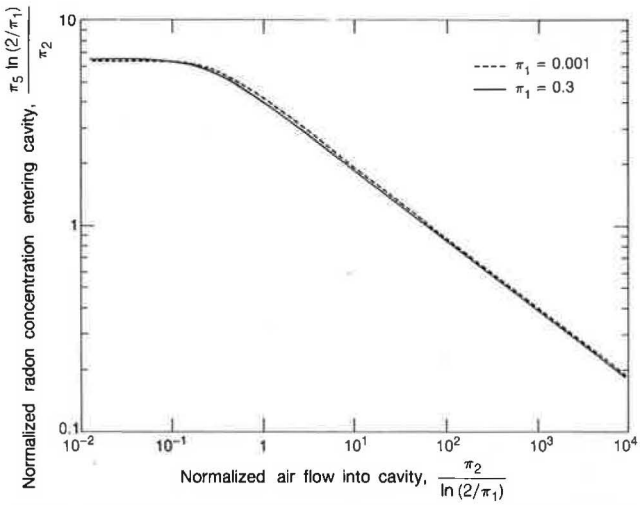

Figure 4. Normalized radon concentration entering a cylindrical cavity under steady-state conditions vs the normalized rate of air flow into the cavity. With the normalization shown here, the results are essentially independent of cavity diameter.

lead to high ^{222}Rn entry rates. Examples (e.g., ref 19) of such penetrations include these: a perimeter drain tile system connected to a basement sump through an untrapped pipe, a "French drain" (i.e., a designed gap of several centimeters width between the wall and the floor), and the shrinkage crack along the floor–wall joint of a basement with concrete floor and walls. Such penetrations may serve as a major conduit for ^{222}Rn entry.

These pathways may reasonably be modeled as a buried cylindrical cavity with a horizontal axis. The length of the cavity is approximated by the perimeter length of the basement; its radius is estimated to be the radius of the drain pipe in one case or half the width of the gap or crack in the others. Since the length of the cavity is typically much greater than the other length scales, the problem is analyzed in two dimensions, neglecting end effects.

This case is distinguished from the spherical cavity primarily in the change from three-dimensional to two-dimensional flow. As a consequence, for a given value of Π_1, the trajectory travel times and rate of dynamic pressure drop with distance from the cavity surface are much smaller for the cylindrical case. (See Figure 3 and note that the values of τ are given for $\Pi_2 = 1$, rather than for $\Pi_2 = 100$ as in Figure 1.)

By analyzing this configuration, a basis is provided for relating the results obtained from the probe to cases of interest for ^{222}Rn entry into houses.

Analysis. With the change in geometry, two of the dimensionless groups must be altered. Radon flux and air flow into the cavity are given per unit length of cavity, and the normalized parameters are designated Π_5 and Π_6, respectively. (See Table I.)

For this geometry, the Laplace equation is conveniently solved by using bipolar coordinates (*16*). In terms of the dimensionless groups, the flow rate into the cavity is given by

$$\Pi_6 = \frac{2\pi}{\sinh^{-1}\{[\{1/\Pi_1\}^2 - 1]^{1/2}\}} \tag{17}$$

For $\Pi_1 \ll 1$, $\Pi_6 \rightarrow 2\pi/[\ln(2/\Pi_1)]$.

The normalized radon flux into the cavity is determined in a manner that is analogous to that for the spherical cavity, as described in the previous section.

Results. The normalized radon concentration entering the cylindrical cavity is shown in Figure 4 as a function of the normalized rate of air flow into the cavity. As in the case of the spherical cavity, there are two zones of interest. For small rates of air flow into the cavity, i.e. $\Pi_2 < 0.1 \ln(2/\Pi_1)$, the radon flux is proportional to the dynamic pressure difference:

$$F = 2\pi GL\Delta P_o k/\mu\lambda \ln(2H/r) \tag{18}$$

where r is half the width of the gap or crack.

For high rates of air flow into the cavity, the radon concentration at the cavity surface is depleted because of the short time of transit of air parcels through the soil relative to the radon half-life. In this regime, the radon entry rate is given by

$$F = 4.0GLH^{2/3}\epsilon^{1/3}\left[\frac{\Delta P_o\, k}{\mu\lambda \ln(2H/r)}\right]^{2/3} \tag{19}$$

The depletion regime occurs under the condition $\{\Delta P_o\, k\} > \{0.5\, \epsilon\, \mu\, \lambda\, H^2 \ln(2H/r)\}$. (For the representative conditions of $\epsilon = 0.5$, $H = 2$ m, $r = 7.5$ cm, and $\Delta P_o = 4$ Pa, this condition becomes $k > 3.5 \times 10^{-11}$ m^2.) Because the presence of the basement walls shields a portion of the flow, it is expected that the actual rate of ^{222}Rn entry into a building under these conditions would be in the range 50–100% of that predicted for the idealized geometry considered here.

If the interior of the building can be treated as a single, well-mixed volume, and if the radon entry rate from soil is equal to the radon source potential, then the indoor radon concentration, I, is given by

$$I = \frac{I_o + (F/V) + S}{\lambda + (Q_v/V)} \tag{20}$$

where I_o is the outdoor radon concentration, V is the building volume, S is the rate of entry of radon from sources other than soil and outdoor air, such as building materials and potable water (*8*), and Q_v is the flow rate of outdoor air into the building. Generally, the radon decay rate, λ, is much smaller than Q_v/V. In cases of present interest, where F is large, radon entry from sources other than the soil may be neglected. Under these conditions, eq 20 reduces simply to $I = F/Q_v$.

A high ^{222}Rn source potential might be considered one that yields a predicted indoor radon concentration for a representative house exceeding a particular guideline. The U.S. Environmental Protection Agency has recommended a limit of 150 Bq m^{-3} (4 pCi L^{-1}) as an annual average ^{222}Rn concentration in the living space of houses (*20*). The volume of a house with one floor plus a full basement and

Table II. Comparison of Measured Indoor ^{222}Rn Source Potential and Observed ^{222}Rn Concentrations in the Basement of Several Houses

house–probe no.	radon source potential[a]					$[^{222}Rn]$,[d] Bq m^{-3}
	ΔP,[b] Pa	k, m^2	I, Bq m^{-3}	ϵG, Bq m^{-3} s^{-1}	F,[c] Bq s^{-1}	
1–1	50	2.7×10^{-11}	2.7×10^4	0.025	4–8	925
2–1	10	3.3×10^{-10}	1×10^6	0.9	930–1600	7600
2–2	10	7×10^{-10}	4×10^5	0.4	680–1200	
2–3	250	5.4×10^{-12}	4×10^6	3.6	120–280	
3–1	50	1.1×10^{-11}	1.2×10^5	0.11	8–17	850
3–2	10	7×10^{-10}	7.7×10^4	0.10	170–290	
3–3	50	1.7×10^{-11}	5×10^4	0.05	5–11	
4–1	500	1.7×10^{-12}	1.2×10^4	0.02	0.2–0.5	100
4–2	500	1×10^{-12}	4.4×10^3	0.01	0.06–0.14	

[a] ΔP is the dynamic pressure difference applied between the soil surface and the soil cavity; k is the measured soil permeability; I is the measured radon concentration in the sample of air extracted from the soil; ϵG is the measured product of soil porosity and the radon generation rate, and F is the calculated radon source potential. [b] The value of ΔP was selected to be as small as could be stably maintained and yield an accurately measurable flow rate. For moderately permeable soils ($k >$ ca. 10^{-11} m^2, in practice), ΔP = 10–50 Pa, whereas for low permeability soils it was necessary to have ΔP = 250–500 Pa to produce a readily measured flow rate. [c] Range of values computed by assuming r = 0.05–7.5 cm and ϵ = 0.5. [d] Measured in the basement.

a perimeter of 40 m might be 450 m^3. If we assume that the interior volume is well-mixed and that the ventilation rate is a typical value of 0.5 vol/h (i.e., Q_v = 225 m^3 h^{-1}), an entry rate of 9.3 Bq s^{-1} would yield an indoor concentration exceeding the guideline. Thus, 10 Bq s^{-1} is the approximate value of the indoor ^{222}Rn source potential of a soil that would justify concern about nearby indoor radon concentrations.

Experimental Measurement of the ^{222}Rn Source Potential

Measurement Techniques. The instrumentation consisted of probes made of galvanized metal pipe, a set of diaphragm gauges (Magnehelic, Dwyer Instruments, Inc., Michigan City, IN) for measuring differential pressures in the range of 10–500 Pa, a set of rotameters for measuring air flow in the range of 1–3000 cm^3 min^{-1}, radon concentration measurement apparatus, a control valve, and a pump.

The probes had an inside diameter of 0.6 cm and a length of 1.5 or 2 m. To install a probe, a slightly undersized pilot hole (~1.2-cm diameter) was drilled in the soil to the desired depth. An installation rod was inserted into the probe, and the unit was hammered into the pilot hole. The diameter of the rod was slightly smaller than the inner diameter of the probe, and it extended 2 cm beyond the probe length. At the top of the rod was a 2.5-cm-diameter cylinder which served as the hammering surface. After the installation rod was removed, a small auger was used to ensure that the soil at the bottom of the pocket created at the tip of the probe was not compacted.

The top of the probe was then coupled to the pressure and flow instrumentation. Flows were usually measured at differential pressures of 10 or 50 Pa, the lower value being used if it could be stably maintained. In those cases where soil permeabilities were low (i.e., below ca. 10^{-11} m^2), differential pressures of 250 or 500 Pa were used.

Measurement of the radon concentration in the extracted soil gas was made with a ~250-cm^3 flow-through scintillation cell and a portable photomultiplier-tube-based counting system (Type 300 and Model RM-1003, respectively, Pylon Electronic Development Co., Ottawa, Canada). Approximately one-half to several liters of soil gas were extracted initially, depending on the soil permeability and the time required for the permeability measurement. The scintillation cell was then closed and 10 min allowed to elapse before counting the α decays due to radon in the cell. This time period was sufficient to allow decay of any of the shorter lived ^{220}Rn that is also present in the soil gas. The observed α decays were converted to ^{222}Rn gas concentration, correcting for background and for α decays due to radon progeny that build up from the radon in the cell.

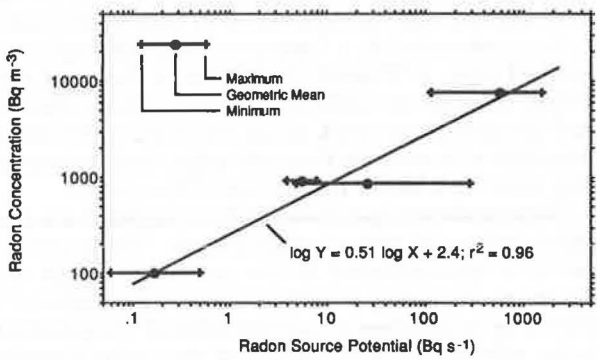

Figure 5. Indoor radon concentration measured in the basement vs radon source potential of soil measured at four New Jersey homesites. The regression line relates the logarithm of the measured indoor radon concentration (Y) to the logarithm of the geometric mean radon source potential (X) measured at each site.

To obtain the most reliable results, the measurements should be carried out during a period when the barometric pressure is relatively stable (it is particularly important to avoid a period of sharply rising pressure), and not during or immediately after a heavy rainfall. In addition, the measurements should be made beyond a distance x from any building, where x is approximately 2 times the depth below grade of the lowest floor of the building, as the soil gas radon concentration near a building may be depleted by air flow through the building's substructure.

Measurement Results. Measurements were made at several homes in New Jersey that were part of a year-long, intensive study conducted by Lawrence Berkeley Laboratory on radon entry and control (*21*). Results are shown in Table II for three of these homes along with a fourth home (*22*) selected because it had low radon concentrations in the basement and therefore the soil at that site might be expected to have a low radon source potential.

The ^{222}Rn source potential was computed for these houses by using eq 18 and 19, the measured radon generation rate and permeability, and the nominal geometry and pressure difference given under Radon Source Potential. The resulting source potentials vary by more than

3 orders of magnitude and correlate well with the observed radon concentrations in the basements of these houses (see Figure 5). The significant variability in source potential at a given site suggests that measurements should be made at several locations at a site to reduce the influence of an anomalous measurement.

Discussion

To recapitulate, a method is proposed for assessing the potential of soil to generate high indoor radon concentrations in buildings constructed upon it. The method is comprised first of a procedure for measuring the permeability of soil and the generation rate of radon in the soil pores and second of a means of interpreting the results to predict the maximum sustainable rate of entry via soil gas flow into the substructure of a building having characteristics representative of a single-family residence. In a small, preliminary sample, the method is shown to yield results that correlate well with indoor concentrations.

Key issues require further evaluation before the assessment method presented in this paper can be considered a valid means of determining the radon source potential of soil. One such issue is the extent to which the description of radon migration and entry adopted here prevails in the housing stock. Other scenarios may also be important in accounting for elevated concentrations. For example, if the soil near a house has substantially nonuniform permeability, then radon may diffuse from low-permeability zones to areas of higher permeability and subsequently be carried by soil gas flow into the structure. In such a case the entry rate may depend upon the diffusion coefficient of radon in the soil, a factor not considered here. It will also depend in such a case upon the detailed geometry both of the high-permeability zones and of the coupling between the building substructure and the soil. Such a condition might be detected with the present technique by observation of large permeability variations with small changes in probe location.

As a related matter, the combination of building substructure and entry pathway considered in this paper is only one of several specific possibilities, all of which may be important. The alternatives include a basement with a penetration through a slab floor that is underlain by a gravel layer, a basement with concrete-block walls, a slab-on-grade foundation, or an unvented unpaved crawl space. It will require considerable further work to assess the radon source potential for these specific substructure conditions. However, predictions for these alternatives are likely to differ from the case considered in this paper only by a fraction of an order of magnitude, and given that the ^{222}Rn source potential varies by more than 3 orders of magnitude it seems reasonable to use the present pathway description until the other cases are analyzed.

Another issue is the degree of soil inhomogeneity at a house site—both laterally and with depth in the soil—and its concomitant influence on the measurement of soil characteristics used to determine the radon source potential. In some cases, soil permeability and radon content have been observed to be relatively homogeneous (*23*), in which case a few measurements (or even one) will suffice. In other cases, widely varying permeability and soil gas radon concentrations have been observed (*21*); in such cases, the usefulness of these measurements for estimating potential radon entry rates is likely to be reduced.

Further work to improve the probe system appears warranted. The analysis represented by Figure 1 suggests that the measurement results are highly sensitive to soil conditions within a few probe diameters of the cavity. The present installation techniques may significantly disturb the soil within this range. In addition, the cavity in the present system is only a crude approximation to an isolated sphere. The use of alternative probe geometries should be investigated.

Another issue not addressed in the present work is the temporal variability in the ^{222}Rn source potential. Variations in moisture content of the soil could potentially cause large variations in both the radon generation rate, by altering the emanating fraction, and the soil permeability. Experimental study of the magnitude of this effect would be useful.

Most importantly, further survey work must be conducted comparing measured indoor radon concentrations with the indoor ^{222}Rn source potential of the nearby soil. Ultimately, the demonstration of a strong empirical correlation between the higher observed indoor concentrations and the source potential is both sufficient and necessary to justify the use of this method for appraising the risk of high indoor ^{222}Rn concentrations from soil.

Acknowledgments

Discussions with N. H. Brooks contributed substantially to the development of this work. Comments by W. Fisk led to improvements in the manuscript.

Registry No. Radon-222, 14859-67-7.

Literature Cited

(1) Bruno, R. C. *J. Air Pollut. Control Assoc.* **1983**, *33*, 105–109.
(2) Nero, A. V.; Nazaroff, W. W. *Radiat. Prot. Dosim.* **1984**, *7*, 23–39.
(3) Nero, A. V.; Schwehr, M. B.; Nazaroff, W. W.; Revzan, K. L. *Science* **1986**, *234*, 992–997.
(4) Peake, T. R. Presented at the Fourth International Symposium on the Natural Radiation Environment, Lisboa, Portugal, December 7–11, 1987.
(5) Swedjemark, G. A. *Health Phys.* **1986**, *51*, 569–578.
(6) Eaton, R. S.; Scott, A. G. *Radiat. Prot. Dosim.* **1984**, *7*, 251–253.
(7) Tanner, A. B. In *Geologic Causes of Natural Radionuclide Anomalies: Proceedings of the GEORAD Conference*; Marikos, M. A., Hansman, R. H., Eds.; Division of Geology and Land Survey Special Publication No. 4; Missouri Department of Natural Resources: Rolla, MO, 1988; pp 139–146.
(8) Nazaroff, W. W.; Moed, B. A.; Sextro, R. G. In *Radon and Its Decay Products in Indoor Air*; Nazaroff, W. W., Nero, A. V., Eds.; Wiley: New York, 1988; Chapter 2.
(9) Nazaroff, W. W.; Lewis, S. R.; Doyle, S. M.; Moed, B. A.; Nero, A. V. *Environ. Sci. Technol.* **1987**, *21*, 459–466.
(10) Clements, W. E. Ph.D. Thesis, New Mexico Institute of Mining and Technology, Socorro, NM, 1974.
(11) Houseworth, J. E. Ph.D. Thesis, California Institute of Technology, Pasadena, CA, 1984.
(12) Bear, J. *Dynamics of Fluids in Porous Media*; American-Elsevier: New York, 1972; p 126.
(13) Nazaroff, W. W.; Feustel, H.; Nero, A. V.; Revzan, K. L.; Grimsrud, D. T.; Essling, M. A.; Toohey, R. E. *Atmos. Environ.* **1985**, *19*, 31–46.
(14) Schery, S. D.; Gaeddert, D. H.; Wilkening, M. H. *J. Geophys. Res.* **1984**, *89*, 7299–7309.
(15) Fukuda, H. *Soil Sci.* **1955**, *79*, 249–256.
(16) Morse, P. M.; Feshbach, H. *Methods of Theoretical Physics*; McGraw-Hill: New York, 1953; Part I, Chapter 5, and Part II, Chapter 10.
(17) Rogers, V. C.; Nielson, K. K.; Kalkwarf, D. R. *Radon Attenuation Handbook for Uranium Mill Tailings Cover Design*; U.S. Nuclear Regulatory Commission: Washington, DC, 1984; NUREG/CR-3533.
(18) Press, W. H.; Flannery, B. P.; Teukolsky, S. A.; Vetterling, W. T. *Numerical Recipes: The Art of Scientific Computing*; Cambridge University Press: Cambridge, England, 1986; Chapter 15.

(19) Scott, A. G. In *Radon and Its Decay Products in Indoor Air*; Nazaroff, W. W., Nero, A. V., Eds.; Wiley: New York, 1988; Chapter 10.
(20) U.S. Environmental Protection Agency *A Citizen's Guide to Radon*; U.S. EPA: Washington, DC, 1986; OPA-86-004.
(21) Sextro, R. G.; Harrison, J.; Moed, B. A.; Revzan, K. L.; Turk, B. H.; Grimsrud, D. T.; Nero, A. V.; Sanchez, D. C.; Teichman, K. Y. In *Indoor Air '87: Proceedings of the 4th International Conference on Indoor Air Quality and Climate*; Seifert, B., Esdorn, H., Fischer, M., Rüden, H., Wegner, I., Eds.; Institut für Wasser-, Boden- und Lufthygiene: Berlin, 1987; Vol. 2, pp 295–299.
(22) Sextro, R. G., Lawrence Berkeley Laboratory, unpublished data, 1987.
(23) Sextro, R. G.; Moed, B. A.; Nazaroff, W. W.; Revzan, K. L.; Nero, A. V. In *Radon and Its Decay Products: Occurrence, Properties and Health Effects*; Hopke, P. K., Ed.; ACS Symposium Series 331; American Chemical Society: Washington, DC, 1987; pp 10–29.

Received for review June 9, 1988. Accepted November 8, 1988. This work was supported by the Director, Office of Energy Research, Office of Health and Environmental Research, Human Health and Assessments Division and Pollutant Characterization and Safety Research Division, and by the Assistant Secretary for Conservation and Renewable Energy, Office of Building and Community Systems, Building Systems Division of the U.S. Department of Energy (DOE) under Contract No. DE-AC03-76SF00098. It was also supported by the Office of Radiation Programs, of the U.S. Environmental Protection Agency (EPA) through Interagency Agreement DW89932609-01-0 with DOE. This manuscript has not been subjected to EPA review. Its contents do not necessarily reflect the views of EPA. Mention of firms, trade names, or commercial products do not constitute endorsement or recommendation for use.